




# Cryopurification and a Microbial Fuel Cell Process as a Combined Approach to Treat Mine-Impacted Water (Faro Mine, Yukon, Canada)

Ethan Allen<sup>1</sup> · Daria Popugaeva<sup>1,2</sup> · Carlos Munoz-Cupa<sup>2</sup> · Amarjeet Bassi<sup>2</sup> · Konstantin Kreymann<sup>2</sup> · Ajay K. Ray<sup>2</sup> 

Received: 14 November 2023 / Accepted: 16 August 2024 / Published online: 30 August 2024  
© The Author(s) under exclusive licence to International Mine Water Association 2024

## Abstract

A water treatment approach integrating freezing technology, also referred to as cryopurification, and a microbial fuel cell (MFC) process was tested for Zn removal in laboratory experiments. The water samples used were from the Faro Mine site, in Yukon, Canada. The effect of freezing temperature, mixing, and the direction of the ice front propagation on Zn removal from the Faro Mine water was investigated and quantitatively analyzed. The MFC was used to treat the post-cryopurification brine. When the coolant temperature ranged from  $-5$  to  $-1$  °C and 180 rpm solution mixing was used, up to 80–95% of the Zn was removed after a single freezing cycle. The results of laboratory experiments demonstrated that Zn concentrations in mine water can be reduced by cryopurification to 0.5 mg/L (the effluent quality standard) under optimal experimental conditions. The MFC process was run for 120 h to test the capacity of the microorganism (*Shewanella oneidensis*) for Zn removal from the brine concentrated by freezing. In these laboratory experiments, MFC showed a reliable and high Zn removal up to 90–93% with *S. oneidensis* incubated in the anode chamber. The MFC generated a maximum power density and open-circuit voltage of 8.8 mW/m<sup>2</sup> and 168.5 mV, respectively.

**Keywords** Northern regions · Zinc removal · Freezing technology · MFC

## Introduction

Freeze concentration, a nature-inspired water treatment technology, also referred to as freeze desalination or cryopurification, is a promising technology for contaminated water treatment (Najim 2022; Yin et al. 2017). The process relies on the principle that the structure of ice crystals does not accommodate impurities/salts meaning that they are rejected by the growing ice as water freezes (Shone 1987). The ice produced by cryopurification is separated from the concentrated solution and then melted to obtain pure water (Najim 2022). Cryopurification has several benefits over other common water treatment and desalination methods (Najim and Krishnan 2023). The energy consumption comparison between cryopurification and conventional evaporative

technology showed that cryopurification is energetically favored by about 70%, and even more near the polar regions where a natural weather advantage exists (Najim 2022; Najim and Krishnan 2022; Xu et al. 2022). Most importantly, little to no chemicals are involved in the process of water treatment by freezing and the cost is half to one tenth that of other methods such as reverse osmosis, evaporative methods, nanofiltration, and distillation, according to available literature data (Xu et al. 2022; Youssef et al. 2014).

Based on laboratory tests and field data, freezing technology is capable of effectively removing several impurities from wastewater and mine-impacted water, including metals such as nickel, cobalt, manganese, and chromium (Hasan and Louhi-Kultanen 2016; Melak et al. 2016; Popugaeva et al. 2021, 2023; Liu et al. 2022; Wijewardena 2018). Among cryopurification cons, a concentrated solution (brine) is produced by the cryopurification process that could harm the environment due to its high contaminant concentration. As an alternative, brine treatment promotes the reduction of pollution, minimization of waste volume, and production of freshwater with high recovery rates. Cryopurification can be combined with other water purification methods, for example, with membrane distillation. Such hybridization

✉ Ajay K. Ray  
aray@eng.uwo.ca

<sup>1</sup> Core Geoscience Services Inc., 4109 4th Ave, Suite 206, Whitehorse, YT Y1A 1H6, Canada

<sup>2</sup> Department of Chemical and Biochemical Engineering, University of Western Ontario, London, ON N6A 5B9, Canada

(integration of cryopurification with other water treatment methods) has the potential to make cryopurification more beneficial. In addition, the process can also be integrated with biochemical processes such as a microbial fuel cell (MFC). A MFC is a process that uses bio-electrochemical processes for voltage generation and has the potential for removing metals. The system uses organic substrates and the microorganism's catalytic activity to generate electricity (Dutta and Kundu 2018). Single-chamber and dual-chamber MFCs are the main configurations of MFCs. The first is also known as an air cathode MFC; it has one chamber for microbial degradation and one cathode that is exposed to air. The second type has two chambers; the anode processes the organic matter and the cathode is exposed to catholyte solutions such as potassium ferricyanide. The two chambers are separated by a proton exchange membrane (Logan 2008; Munoz-Cupa et al. 2021; Obileke et al. 2021). Single-chamber MFCs have been used to remove cadmium, chromium, zinc, and copper from mining wastewater. (Abourached et al. 2014; Peng et al. 2017; Vélez-Pérez et al. 2020; Wang et al. 2016; Xie et al. 2020), while dual-chamber MFCs have been used to recover cadmium, copper, and vanadium (Aiyer 2020). Also, zinc was removed in the cathode chamber (Fradler et al. 2014). Inorganic sulfur compounds in mining wastewater have also been investigated for electricity generation using MFC technology (Ni et al. 2016; Sulonen et al. 2014;). Furthermore, mining wastewater has been treated in a dual-chamber MFC using catholyte reduction in the cathode chamber with different mixtures of microbial cultures in the anode chamber (Ai et al. 2020; Alexandre et al. 2022). These processes emphasize the treatment of organic and sulfur compounds in mining wastewater.

In addition, bacterial cultures for metal remediation have been found in the Yukon Territory. Some of these microorganisms are anaerobic and interact with metal fixation in soils from Zn-Pb deposits (Gadd et al. 2017; Nielsen et al. 2019). The main cultures used and found in Canada's northern territories are composed of sulfate-reducing bacteria, such as *Acidithiobacillus ferrooxidans*, *Pseudomonas putida*, *Bacillus subtilis*, and *Desulfovibrio desulfuricans*, which can be used for the removal of different metals such as iron and chromium (Dixit et al. 2015; Makhallanyane et al. 2016). Other microorganisms with metal-reducing characteristics have been investigated, such as *Geobacter* and *Shewanella oneidensis*. *S. oneidensis* is a gram-negative bacterium that uses extracellular electron transport (EET) for metal removal and bioelectrochemical processes such as MFC. Additionally, *S. oneidensis* is a facultative bacterium that can grow under aerobic and anaerobic conditions, which facilitates its use in different environmental conditions (Min et al. 2017; Yin et al. 2022).

In this work, water from the Faro Mine was used as a feed solution to test a novel approach to mine-impacted water

treatment: cryopurification in combination with the MFC process for zinc removal. Based on a critical analysis of earlier studies, this water treatment approach could offer advantages over conventional treatment approaches, including energy efficiency, no chemical pre-treatment, and zero waste generation (i.e. brine). Notably, this approach could be especially beneficial in colder climates that naturally promote cryopurification. The Faro Mine water has zinc concentrations that are up to almost 25–30 times the effluent quality standard of 0.5 mg/L (The Government of Canada 2022). Taking this into account, the objectives of this research work were to: (i) remove zinc from the Faro Mine water in a set of laboratory experiments using cryopurification to less than or close to the effluent quality standard, and (ii) eliminate the waste product of the cryopurification experiments (i.e. the brine) by treating the brine solution using the MFC process. It was anticipated that this approach could be a sustainable water treatment solution at the Faro Mine site or at other mine and industrial sites in Canada's North.

## Materials and Methods

### Study Area

The feed water used for the laboratory experiments was received from the Faro Mine site (Fig. 1). The Faro Mine is a legacy abandoned mine located in south-central Yukon (62.3527° N, 133.4054° W), near the town of Faro. The site is located on the traditional territory of the Kaska Nations, upstream from the Selkirk First Nation (Crown-Indigenous Relations and Northern Affairs Canada 2021). The physico-chemical properties of the mine-impacted water are shown in Table 1. The water has circumneutral pH and elevated zinc concentrations (Popugaeva et al. 2023; The Government of Canada 2022), which is one of the primary concerns with regard to its impact on sensitive receiving environments in the study area.

### Proposed and Tested Water Treatment Approach for Zinc Removal

In this study, cryopurification was merged with the MFC process for the first time to investigate the effectiveness of this joint treatment on zinc removal from mine-impacted water. Figure 2 illustrates the schematic design of the laboratory setup for the proposed hybrid approach. The left block describes the cryopurification of the mine-impacted water, while the right block (the MFC) was to treat the brine solution produced by the cryopurification experiments. The feed water was first treated by cryopurification and purified water was produced from the melted ice. Subsequently, the brine produced by cryopurification was sent to the anode of the

**Fig. 1** The location of the Faro Mine Complex (Yukon, Canada)



**Table 1** The characteristics of the Faro Mine's water

Parameters	Units	Value
Zinc (total)	mg/L	13.7
pH	N/A	7.2
Salinity	ppt	0.9
Total dissolved solids (TDS)	g/L	1.2

N/A not applicable

dual-chamber MFC; after 120 h of processing time, the bacteria were separated from the anode solution with the brine by centrifugation.

For the cryopurification experiments, a circulating chiller (bath work area dimensions 16.8 × 7.8 × 15.2 cm) was filled with ethylene glycol/water fluid (Cole-Parmer, Vernon Hills, Illinois, USA) that maintains a temperature from −25 to 100 °C. For the MFC experiments, *S. oneidensis* MR-1 was cultivated from ATCC<sup>®</sup>, catalog № 700550<sup>™</sup> (Virginia, USA) using tryptic soy broth at 30 g/L for 24 h at 30 °C. To avoid bacterial contamination, the media and the solutions were sterilized using an autoclave at 121 °C and 15 psi. The bacterial growth was evaluated using a UV spectrophotometer at an optical density (OD) of 600 nm.

The samples collected during the experiments were analyzed for zinc concentrations using an inductively coupled plasma (ICP) instrument. The parameters of the

feed solution, brine, and melted iced (treated solution) were measured using water quality multimeters. The main instruments used for the laboratory experiments are listed in Table 2.

## Laboratory Setup and Methods

### Cryopurification and Data Acquisition

Lab-scale cryopurification experiments were conducted using the set-up shown in Fig. 3a to examine the effects of ice front propagation, cooling temperature, and water mixing on zinc removal. Three cylindrical vessels were used in the experiments and ice shapes of different geometries were produced by each vessel. The vessel that produced glass-like ice shapes (Fig. 3b) was made from stainless-steel. Within this vessel, a freezing front spread from the stainless-steel walls and bottom. To eliminate heat flux through the bottom of vessel #2, which produced pipe-like shapes of ice (Fig. 3c), an additional layer of cork was added. In this vessel, a freezing front spread radially from the stainless-steel walls to the center. Vessel #3, a plastic cylinder with insulated walls and a bottom, produced a solid block of ice when the freezing front propagated top-down (Fig. 3d). In most cases, laboratory experiments were done in triplicate.

In the current study, the laboratory cryopurification experiments procedure described by Popugaeva et al. (2023)

**Fig. 2** Schematic design diagram of two main blocks of laboratory setup

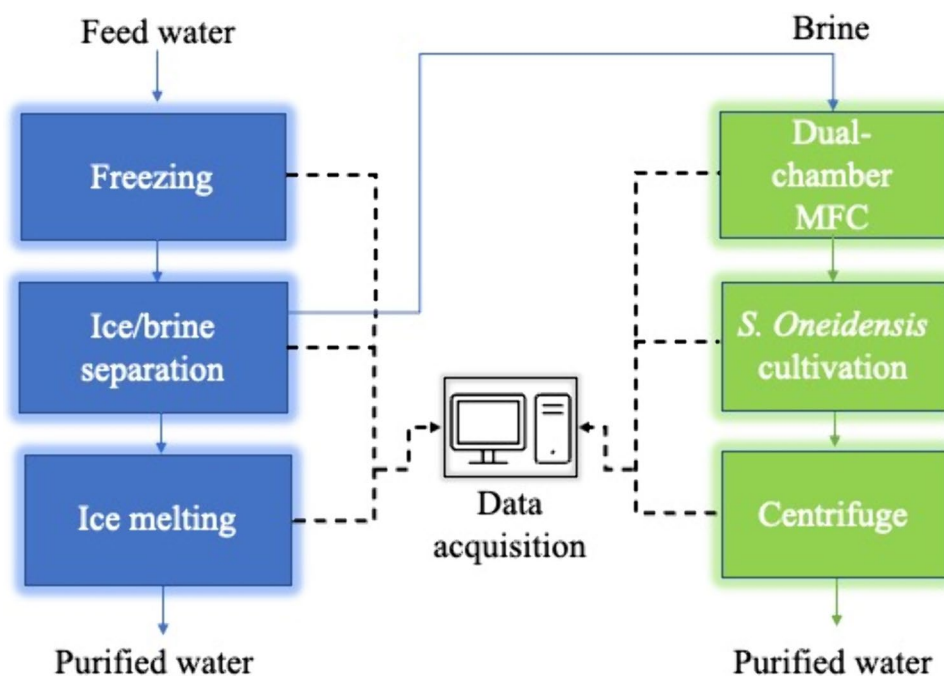


**Table 2** Main instruments used in the laboratory study

Instrument	Accuracy	Supplier
Circulating chiller NESLAB RTE-7	0.1 °C	Thermo Scientific (New Hampshire, USA)
Conductivity, salinity, and total dissolved solids meter	1%	OMEGA, (Connecticut, USA)
Data logger multimeter	0.5% ± 2	Owon OW18 Series (Zhangzhou, China)
Digital thermometer with a temperature probe	0.05 °C	Traceable® (Texas, USA)
ICP	0.01 mg/L	Bureau Veritas (Ontario, Canada)
Data acquisition software	N/A	Traceable® (Texas, USA)
Magnetic stirrer mixer	N/A	VWR (Alberta, Canada)
Electric overhead stirrer mixer	N/A	Vevor (California, USA)
Centrifuge	N/A	Thermo Scientific (USA)

N/A not applicable

was followed. Experiments were conducted in a cooling temperature range of  $-15$  to  $-0.5$  °C. Within vessels #1 and #2, a rectangular agitator was used to investigate the effects of water mixing (180 rpm) on zinc removal from the Faro Mine water. A magnetic stirrer was used for experiments with vessel #3. For a typical cryopurification experiment, 170 mL of Faro Mine water was poured into the vessel and a water sample was taken for zinc testing, temperature, salinity, and TDS testing. The initial temperature of Faro Mine water was maintained at  $10 \pm 1$  °C. An ice fraction (the amount of water converted into ice during the experiments) of  $\approx 35\%$  was used for each experiment as an optimal ice fraction percentage for the cryopurification experiments (Popugaeva et al. 2023).

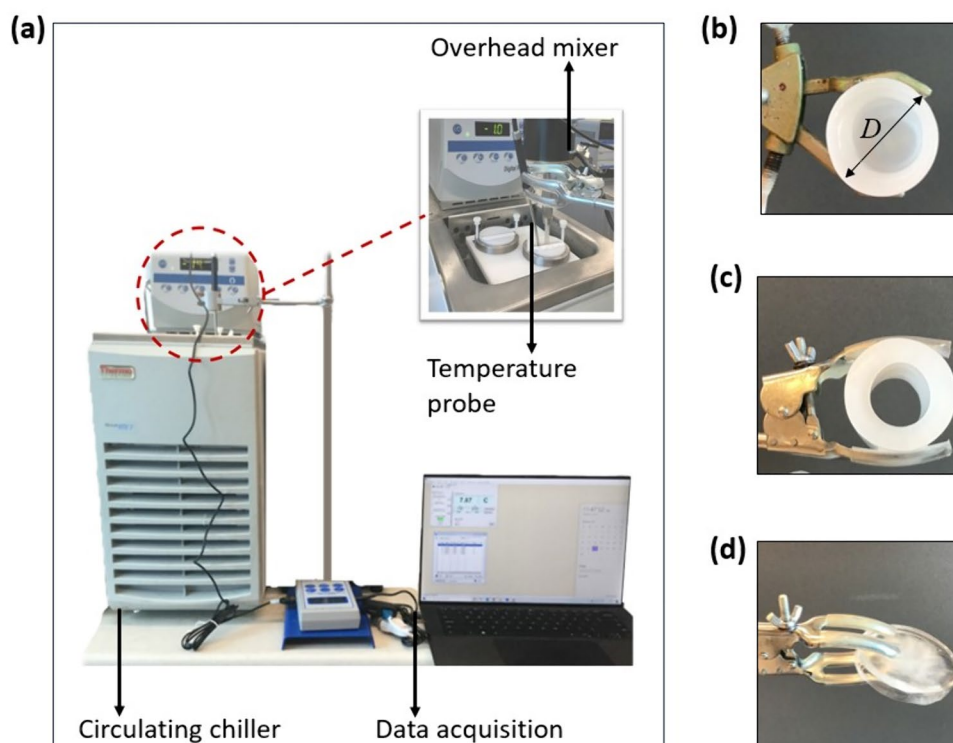
Filled with feed water, vessels #1 and #2 were placed inside the chiller bath at a certain freezing temperature, one

at a time. The water temperature was recorded throughout the experiment every 0.5 minutes using a temperature probe placed  $\approx 2.5$  cm from the vessel wall. After ice reached a target thickness, the freezing process was stopped, and the brine solution was separated from the ice. For a set of experiments with vessel #3, a stainless-steel container with a circulating coolant medium was used as a cooling unit. Vessel #3 was filled with 170 mL of Faro Mine water and a cooling unit was placed at the water surface. Both the vessel and cooling unit were insulated with polyurethane foam from the outside laboratory environment.

A sample of brine and melted ice was collected to record the measurements for temperature, salinity, zinc, and TDS concentration. The purity of the ice produced by cryopurification using vessels #1, #2, and #3 was quantified by comparing zinc concentrations in the melted ice to the initial



**Fig. 3** **a** Laboratory setup and various ice shapes samples produced depending on ice front propagation, **b** freezing from the walls and bottom using vessel #1, **c** freezing from the walls only using vessel #2, and **d** freezing from the top-down using vessel #3. The vessels (ice blocks) diameter,  $D = 5.25$  cm



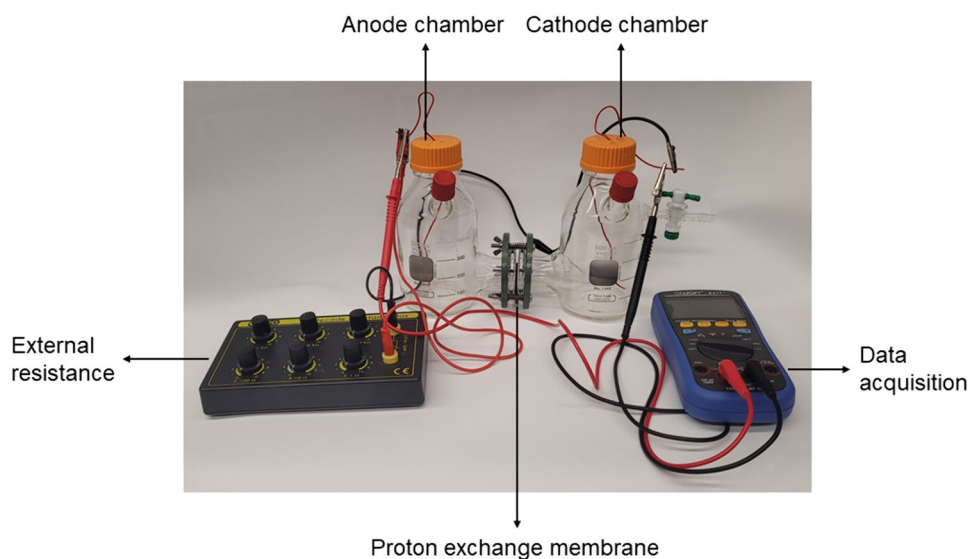
conditions. In the next step, the produced brine was used as a feed solution for a set of laboratory experiments using the MFC process.

### Microbial Fuel Cell Set-Up and Data Acquisition

The MFC setup used in the experimental analysis is shown in Fig. 4. The anode and cathode chambers of the MFC, with a volume capacity of 500 mL each, were separated by

an anion exchange membrane (AXM-100), based on a gel polystyrene cross-linked with divinylbenzene with a thickness of  $0.45 \pm 0.025$  mm and an area of  $36 \text{ cm}^2$ , which was purchased from the Membranes International Inc. (New Jersey, USA). An external resistance of  $1000 \Omega$  connected the anode and cathode chambers. The goal of the MFC experiments was to determine the residual zinc concentration after bacterium cultivation in the anode chamber, while simultaneously generating power.

**Fig. 4** Dual-chamber microbial fuel cell set-up connected through an external resistance and a multimeter



The anode chamber was fed with the brine solution produced by the cryopurification process, followed by the addition of tryptic soy broth (TSB) at 30 g/L, mineral solution (M9, a buffered minimal microbial medium) at 11.3 g/L, and 18 mM sodium lactate. The anode chamber was inoculated with *S. oneidensis* at an optical density  $OD_{600nm}$  of  $0.53 \pm 0.1$ . The temperature ( $T$ ) was kept constant at 30 °C using an incubator with mixing at 80 rpm. 50 mM  $K_3[Fe(CN)_6]$  in a 100 mM phosphate buffer solution (PBS) was the catholyte solution. The voltage output was displayed as the response of the electron transport from the anode to the cathode chamber. The external resistance was changed from 10 to 80,000  $\Omega$  to obtain the polarization curves. The voltage was measured with a multimeter with data logging. The data was stored every hour for 120 h with the addition of TSB and M9 to the anode chamber every 24 h. Watts's and Ohm's laws were used to determine current density ( $I$ ) and power density ( $P$ ) (Logan 2008).

### Evaluation of Zinc Removal Efficiency

The effectiveness of cryopurification for zinc removal from the Faro Mine water was quantitatively estimated using Eqs. (1) and (2) (Miyawaki and Inakuma 2021; Moharramzadeh et al. 2021). The ice fraction was calculated using Eq. (3). A high-quality cryopurification process was achieved when the partition coefficient  $K$  value (Eq. 1) was close to zero and there was a high removal percentage (Eq. 2).

$$K = C_{ice}/C_{brine} \quad (1)$$

$$Removal (\%) = (1 - C_{ice}/C_0) * 100 \quad (2)$$

$$Ice\ fraction(\%) = V_{ice}/V_0 * 100 \quad (3)$$

where  $C_{ice}$  is the zinc concentration in the melted ice (mg/L),  $C_{brine}$  is the zinc concentration in the brine (mg/L),  $C_0$  is the initial zinc concentration in the Faro Mine water (mg/L),  $V_{ice}$  is the volume of melted ice (mL), and  $V_0$  is the initial volume of the Faro Mine water (mL).

For the MFC experiments, total zinc concentration was measured using ICP at three different times (0, 24, and 120 h) after centrifugation of the solution for bacteria separation. Centrifugation was done at 7000 g-force for 20 min, and the supernatant was sampled for zinc analysis. Moreover, the solution was centrifuged at the same conditions to evaluate the zinc uptake by the bacteria after 24 h. The supernatant was collected, and the bacteria cells were resuspended and washed with PBS solution three times. A sonicator was used to break the extracellular membrane. The solution was centrifuged again under the same conditions and the supernatant was then evaluated for total zinc. Zinc removal through the MFC was evaluated analogously to Eq. (2).

## Results and Discussion

### The Effect of Coolant Temperature and Ice Shape

Ice purity is influenced by the cooling rate, which controls ice crystal growth. As the cooling rate increases, contaminant inclusions in the crystal layer may increase (Ila and Louhi-Kultanen 2023). The cooling rate can be controlled by the freezing temperature,  $T_f$ . The effect of  $T_f$  (−15 to −0.5 °C) on the purity of ice at a constant ice fraction ( $\approx 35\%$ ) was investigated in a set of laboratory experiments. According to the results of experiments, the purest ice was produced at the lowest cooling rate when  $T_f$  was −1 to −0.5 °C (Fig. 5). The highest zinc removal, up to 81%, was achieved using vessel #3, while vessel #2 and vessel #1 showed 72 and 57% zinc removal, respectively. Freezing from the top-down (vessel #3) facilitated better contaminant removal than vessels #1, and #2, which can be explained by natural convection that developed under the ice in vessel #3, leading to a better solution mixing and as a result, higher contaminant removal. A similar trend, that freezing from the top-down was more efficient than freezing from the bottom and lateral freezing due to natural convection, was observed in another study (Jayakody et al. 2017).

Natural convection, laminar, and turbulent mixing can all determine the conditions in which ice crystals nucleate and grow, improving the effectiveness of cryopurification (Green 2019). Laboratory experiments on cryopurification could be fulfilled by using various solution movement mechanisms, including, but not limited to natural convection, stirring, circulation due to aeration, and ultrasonic radiation (Samsuri et al. 2016).

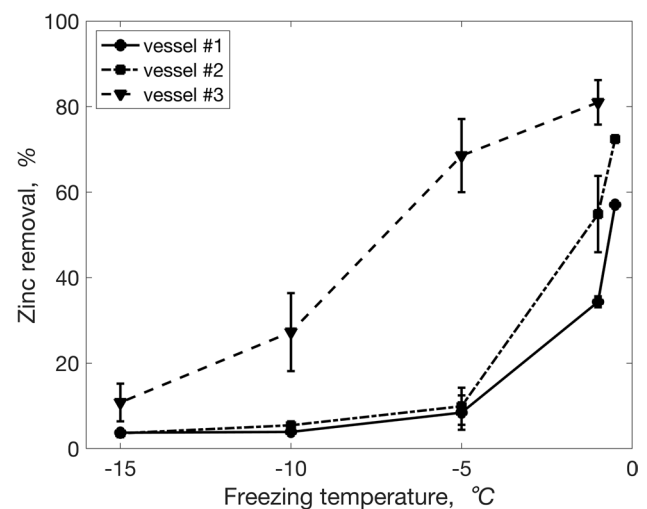


**Fig. 5** The effect of freezing temperature ( $T_f$ ) on the purity of ice at constant ice fraction ( $\approx 35\%$ ) using laboratory vessels

## The Effect of Constant Solution Stirring

The effect of constant mixing at 180 rpm on zinc removal was investigated in the  $T_f$  range of  $-1$  to  $-15$  °C and ice fraction of  $\approx 35\%$  by stirring (Fig. 6). The results of the experiments revealed a notable increase in zinc removal with mixing, reaching up to 92–95%. Removal of up to 35–52% using vessels #1 and #2, respectively, at lower  $T_f$  was achieved. That was greater than in the experiments without mixing. These results were consistent with previous literature findings (Moharramzadeh et al. 2021; Xu et al. 2022) that stirring improved ice purity.

Purer ice was consistently obtained using the top-down freezing in experiments with and without mixing at  $T_f$  from  $-5$  to  $-15$  °C. The removal rates, in general, followed the sequence of vessel #3 > vessel #2 > vessel #1, both with and without stirring (Table 3). Freezing from the top-down in vessel #3 enabled convection, leading to better solution mixing and therefore, greater zinc removal.

Initial zinc concentration and its concentrations in the melted ice and brine solutions were evaluated in each experiment. The distribution of zinc concentrations in various fractions at  $T_f -15$  °C is shown in Fig. 7. Compared to

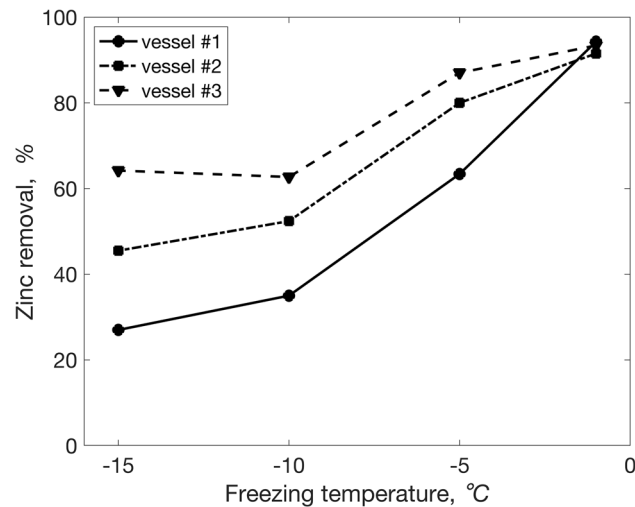


**Fig. 6** The effect of solution stirring on zinc removal. Experimental conditions: stirring speed 180 rpm,  $T_f$  range  $-1$  to  $-15$  °C, ice fraction  $\approx 35\%$

**Table 3** The effects of solution stirring, freezing temperature,  $T_f$  and ice shape on the efficiency of zinc removal based on the calculated partition coefficient,  $K$

$T_f$ (°C)	$K$ , vessel #1		$K$ , vessel #2		$K$ , vessel #3	
	No stirring	Stirring	No stirring	Stirring	No stirring	Stirring
$-1$	0.57	0.03	0.36	0.05	0.16	0.05
$-5$	0.87	0.22	0.87	0.15	0.24	0.09
$-10$	0.94	0.54	0.93	0.36	0.64	0.29
$-15$	0.94	0.63	0.95	0.45	0.87	0.28

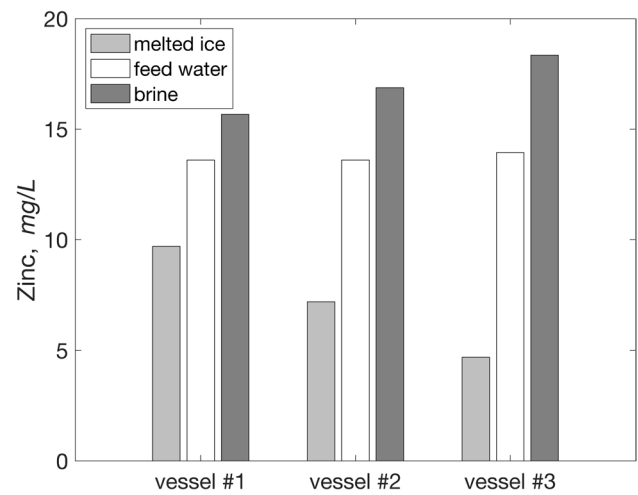


**Fig. 7** Zinc concentration in feed water, melted ice and brine. Experimental conditions:  $T_f -15$  °C, ice fraction  $\approx 35\%$ , mixing speed 180 rpm

zinc concentrations in the raw feed water, the melted ice contained 27–64% less zinc, while zinc concentrations in brine increased by 15–32% depending on the vessel used in the experiment. The melted ice salinity could be decreased from 0.9 to 0.1 ppt while the brine salinity reached up to 1.2–1.3 ppt. A similar trend with TDS concentration was observed; TDS concentration could be decreased from 1.20 to 0.07 g/L in the melted ice and increased to 1.6 g/L in the brine. The brine produced using vessels #2 and #3 at  $T_f$  of  $-1$  °C was used as feed water for the MFC experiments with an average initial zinc concentration of 16.8 and 17.8 mg/L, respectively.

## Microbial Fuel Cell Performance

The power density curve showed a maximum ( $P_{max}$ ) peak at a current density of 63.8 mA/m<sup>2</sup> with a result of 8.80 mW/m<sup>2</sup> (Fig. 8). The optimal external resistance ( $R_{ext}$ ) from the polarization curves was 800  $\Omega$ , corresponding to the maximum power density produced at that external resistance. This was used as the external resistance for the open-circuit voltage (OCV).  $P_{max}$  for the single-chamber MFCs with the removal of cadmium and zinc was 3600 mW/m<sup>2</sup> (Abou-rached et al. 2014), and chromium, copper, and vanadium

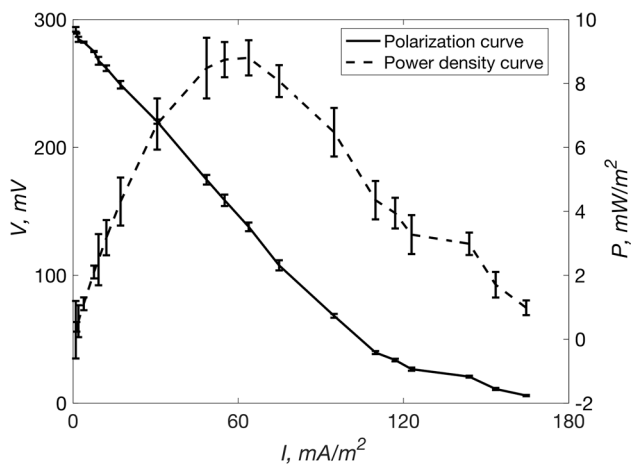


**Fig. 8** Polarization and power density curve evaluated varying the external resistance from 10 to 80,000  $\Omega$  using a dual-chamber MFC

in a dual-chamber MFCs was 138.72 mW/m<sup>2</sup> (Aiyer 2020). Moreover, the use of acid mine drainage in MFCs showed a  $P_{\max}$  of 195.07 mW/m<sup>2</sup>, 51.3 mW/m<sup>2</sup> (Peng et al. 2017), and 400 mW/m<sup>2</sup> (Stefanova et al. 2018). This study showed less power density than other research. However, power density is related to the size and distribution of the electrodes, which in this case were not coated, and the use of conventional copper wires decreased the rate of electron transport through the external circuit. Moreover, the maximum power density determined the internal resistance ( $R_{\text{int}}$ ) because at the maximum point,  $R_{\text{ext}} = R_{\text{int}}$ . At this point, the less potential difference in the MFC made electron transport more efficient.

Additionally, the polarization curve showed a maximum voltage of 292.3 mV (Fig. 8). The polarization curve demonstrates a slope of 1.9, demonstrating the low internal resistance of this system and efficient electron transport. In addition, the polarization curve demonstrates a low loss of mass transfer polarization after 109.9 mW/m<sup>2</sup>, indicating better diffusion of the protons through the membrane. In comparison, a faster decrease in the same zone of mass transfer loss demonstrated greater efficiency in the system (Aiyer 2020). Similarly, the high mass transfer losses showed a fast reduction in electron transport; however, the goethite electrode performed better than the carbon felt electrode used in the following study (Jadhav et al. 2015). Additionally, a high temperature of 40 °C showed a higher power density of 511 mW/m<sup>2</sup> (Stefanova et al. 2018).

Figure 9 shows four different peaks that were related to the feed in the anode chamber every 24 h. In addition, after 36 h, the concentration losses in the OCV were higher though, due to the constant feeding, the reduction was not as high as the control MFC, which was operated with TSB in the anode chamber. However, a higher OCV above 300 mV for zinc removal from the contaminated water in the cathode chamber was previously shown using MFC (Fradler et al.

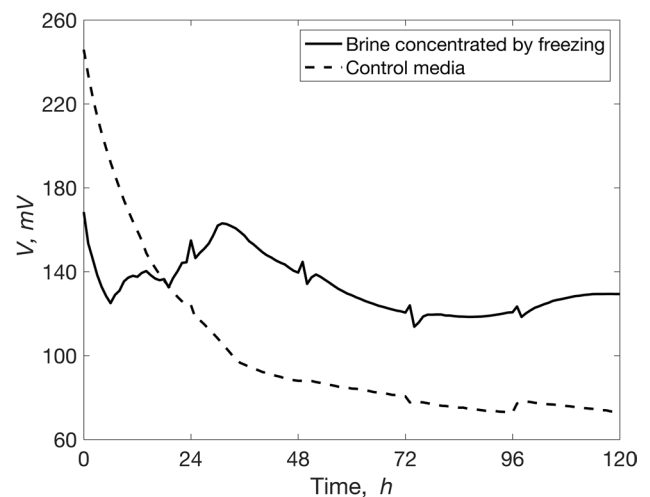


**Fig. 9** Open-circuit voltage evaluated for 120 h with anode feeding every 24 h. Experimental conditions:  $T = 30$  °C, incubator mixing 80 rpm

2014; Lim et al. 2021). The lower OCV in this study could be due to an adverse effect of the contaminated water to the bacterial metabolism, which reduced the electron transport. The control media OCV was less due to the reduced redox potential during the operation because the electron donor was not sufficient for the oxidation process. A higher power density production and more efficient electron transport in the MFC is highly recommended to increase the practical applications of the MFC, such as for biosensors (Hasan et al. 2023; Maqsood et al. 2022). However, due to the low power densities generated, low electron transport, and small electrode surface area, the applicability needs more research (Chaturvedi and Verma 2016). With more studies to scale-up this technology without losing power, the applications of this technology will increase.

### The Effectiveness of the Microbial Fuel Cell in Zinc Removal

Zinc removal was measured at the beginning of the MFC operation, after 24 h, and at 120 h, with a constant temperature of 30 °C (Table 4). The experiments had different initial zinc concentrations corresponding to the two brine solutions obtained at  $T_f - 1$  °C using vessels #2 and #3 and raw feed water (before freezing). The initial zinc concentration influenced the removal efficiency with greater removal at higher initial zinc concentrations, as the results of experiments showed (Table 4). The best removal was 93% in 120 h at an initial zinc concentration of 17.8 mg/L. The greatest removal rate occurred in the first 24 h when the bacterial activity was higher due to their almost exponential growth phase in the brine-concentrated water between 0 and 8 h (Fig. 10).



**Table 4** Zinc removal by MFC with solution fed in the anode chamber

Time (h)	Experiment I (Brine)		Experiment II (Brine)		Experiment III (Raw feed water)	
	Concentration (mg/L)	Removal (%)	Concentration (mg/L)	Removal (%)	Concentration (mg/L)	Removal (%)
0	17.8	N/A	16.8	N/A	13.7	N/A
24	2.4	87	2.3	86	3.0	78
120	1.2	93	1.4	92	1.4	90

N/A not applicable

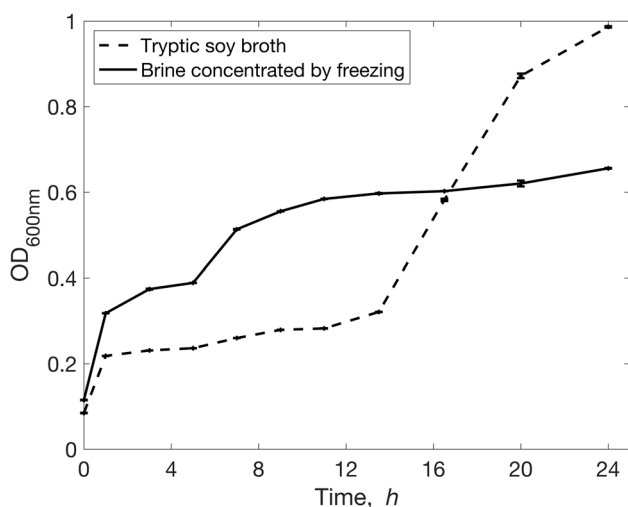


**Fig. 10** *Shewanella oneidensis* growth in brine concentrated by freezing with tryptic soy broth and zinc during the first 24 h of operation. Experimental conditions:  $T = 30\text{ }^{\circ}\text{C}$

The initial concentrations of brine water were 17.8 and 16.8 mg/L, while the initial concentration for the raw feed water was 13.7 mg/L. The bacteria had greater metal absorption (87, 86, and 78% for experiments I, II, and III, respectively) in the almost exponential phase during the first 24 h, based on an analysis of the resuspended metals after treatment of the extracellular membrane. Similarly, Raghad et al. (2016) reported cadmium and lead absorption from wastewater of 64 and 51%, respectively. Additionally, another study reported that a biofilm of *Shewanella xiamenensis* on zeolite had a zinc biosorption of 78% (Zinicovscaia et al. 2020) and 74% (Zinicovscaia et al. 2021). However, the bacterial growth with brine showed a low rate compared with TSB, which was the optimum bacterium media for growth allowing a better nutrient uptake. Additionally, the high concentration of metals increases the toxicity, inhibiting the growth of the bacterium. *S. oneidensis* uses the cytochromes CymA and MtrCAB complex in the extracellular membrane and bacterial nanowires. In addition, MTrC and OmcA cytochromes are terminal reductases for the metal ions

(Yin et al. 2022). These cytochromes are multi-heme proteins with high redox activity that facilitated the EET and metal respiratory pathway (Otero et al. 2019). Moreover, the greater absorption of the bacteria during the first 24 h aided the formation of extracellular proteins (Ge et al. 2022). In addition, *S. oneidensis* growth with the brine concentrated by freezing absorbed 15.9 mg/L during the first 24 h. This was analyzed using cultivation of the bacterium in a media with the zinc at an initial concentration of 16.9 mg/L. However, the higher metal uptake showed less bacterial growth than with tryptic soy broth.

## Conclusions

The proposed approach of cryopurification followed by MFC for post-cryopurification brine treatment could be an environment-friendly approach for treating the highly contaminated water of the Faro Mine in the Yukon Territory, Canada. Based on the results of the current study, zinc concentrations could be reduced close to the effluent quality criteria of 0.5 mg/L, providing a removal of up to 90–95% under optimal conditions. In addition to zinc removal, the approach showed the possibility of power generation using the MFC process. One of the important parts of the proposed treatment approach is that no chemicals were used to purify the water. The aquatic ecosystems of Canada's northern environments are fragile and, if damaged, a long recovery is expected. This, along with the Yukon's cold climate conditions, which would enhance the efficiency of cryopurification, and the local availability of bacterial cultures for metal remediation, could make applying the proposed and tested approach to the Faro Mine site more sustainable and save energy.

**Acknowledgments** Financial support for this research was provided by the Natural Sciences and Engineering Council of Canada (NSERC) along with MITACS and Core Geoscience Services Inc. (CoreGeo) under the NSERC MITACS Alliance grant (Grant R3839A47). We thank CoreGeo for providing us with the Faro Mine water samples and for their constant support and discussions that facilitated this research.

## References

- Abourached C, Catal T, Liu H (2014) Efficacy of single-chamber microbial fuel cells for removal of cadmium and zinc with simultaneous electricity production. *Water Res* 51:228–233. <https://doi.org/10.1016/j.watres.2013.10.062>
- Ai C, Yan Z, Hou S, Zheng X, Zeng Z, Amanze C, Dai Z, Chai L, Qiu G, Zeng W (2020) Effective treatment of acid mine drainage with microbial fuel cells: an emphasis on typical energy substrates. *Minerals* 10:443. <https://doi.org/10.3390/min10050443>
- Aiyer KS (2020) Recovery of chromium, copper and vanadium combined with electricity generation in two-chambered microbial fuel cells. *FEMS Microbiol Lett* 367:fnaa129. <https://doi.org/10.1093/femsle/fnaa129>
- Alexandre LHZ, Pineda-Vásquez TG, Watzko ES, de Oliveira Souza Recouvreur D, Vasconcellos Antônio R (2022) An evaluation of the potential use of microbial fuel cells for energy production and simultaneous acid mine drainage treatment. *Water Air Soil Pollut* 233:399. <https://doi.org/10.1007/s11270-022-05755-x>
- Chaturvedi V, Verma P (2016) Microbial fuel cell: a green approach for the utilization of waste for the generation of bioelectricity. *Biore-sour Bioprocess* 3:38. <https://doi.org/10.1186/s40643-016-0116-6>
- Crown-Indigenous Relations and Northern Affairs Canada (2021) Faro Mine Remediation Project: Yukon. <https://www.rcaanc-cirnac.gc.ca/eng/1480019546952/1537554989037>. Accessed 1 Dec 2023
- Dixit R, Wasiullah, Malaviya D, Pandiyan K, Singh UB, Sahu A, Shukla R, Singh BP, Rai JP, Sharma PK, Lade H, Paul D (2015) Bioremediation of heavy metals from soil and aquatic environment: an overview of principles and criteria of fundamental processes. *Sustainability* 7:2189–2212. <https://doi.org/10.3390/su7022189>
- Dutta K, Kundu PP (2018) Introduction to microbial fuel cells. Progress and recent trends in microbial fuel cells. Elsevier, Amsterdam, pp 1–6
- Fradler KR, Michie I, Dinsdale RM, Guwy AJ, Premier GC (2014) Augmenting microbial fuel cell power by coupling with supported liquid membrane permeation for zinc recovery. *Water Res* 55:115–125. <https://doi.org/10.1016/j.watres.2014.02.026>
- Gadd MG, Layton-Matthews D, Peter JM, Paradis S, Jonasson IR (2017) The world-class Howard's Pass SEDEX Zn-Pb district, Selwyn Basin, Yukon. Part II: the roles of thermochemical and bacterial sulfate reduction in metal fixation. *Miner Depos* 52:405–419. <https://doi.org/10.1007/s00126-016-0672-x>
- Ge C, Huang M, Huang D, Dang F, Huang Y, Ahmad HA, Zhu C, Chen N, Wu S, Zhou D (2022) Effect of metal cations on antimicrobial activity and compartmentalization of silver in *Shewanella oneidensis* MR-1 upon exposure to silver ions. *Sci Total Environ* 838:156401. <https://doi.org/10.1016/j.scitotenv.2022.156401>
- Green DA (2019) Crystallizer mixing: understanding and modeling crystallizer mixing and suspension flow. Handbook of industrial crystallization. Cambridge University Press, Cambridge, pp 290–312
- Hasan M, Louhi-Kultanen M (2016) Water purification of aqueous nickel sulfate solutions by air cooled natural freezing. *Chem Eng J* 294:176–184. <https://doi.org/10.1016/j.cej.2016.02.114>
- Hasan M, Anzar N, Sharma P, Malode SJ, Shetti NP, Narang J, Kakarla RR (2023) Converting biowaste into sustainable bioenergy through various processes. *Bioresour Technol Reports* 23:101542. <https://doi.org/10.1016/j.biteb.2023.101542>
- Ila M, Louhi-Kultanen M (2023) Purification of monoethylene glycol by melt crystallization. *Chem Eng Sci* 272:118601. <https://doi.org/10.1016/j.ces.2023.118601>
- Jadhav DA, Ghadge AN, Ghangrekar MM (2015) Enhancing the power generation in microbial fuel cells with effective utilization of goethite recovered from mining mud as anodic catalyst. *Bioresour Technol* 191:110–116. <https://doi.org/10.1016/j.biortech.2015.04.109>
- Jayakody H, Al-Dadah R, Mahmoud S (2017) Computational fluid dynamics investigation on indirect contact freeze desalination. *Desalination* 420:21–33. <https://doi.org/10.1016/j.desal.2017.06.023>
- Lim SS, Fontmorin JM, Pham HT et al (2021) Zinc removal and recovery from industrial wastewater with a microbial fuel cell: experimental investigation and theoretical prediction. *Sci Total Environ* 776:145934. <https://doi.org/10.1016/j.scitotenv.2021.145934>
- Liu T, Zhang Y, Tang Y, Wang X, Zhao C, Wang N, Liu Y (2022) Application of progressive freeze concentration in the removal of  $\text{Ca}^{2+}$  from wastewater. *J Water Process Eng* 46:102619. <https://doi.org/10.1016/j.jwpe.2022.102619>
- Logan BE (2008) Microbial fuel cells. Wiley, Hoboken
- Makhalanyane TP, Van Goethem MW, Cowan DA (2016) Microbial diversity and functional capacity in polar soils. *Curr Opin Biotechnol* 38:159–166. <https://doi.org/10.1016/j.copbio.2016.01.011>
- Maqsood Q, Ameen E, Mahnoor M, Sumrin A, Akhtar MW, Bhattacharya R, Bose D (2022) Applications of microbial fuel cell technology and strategies to boost bioreactor performance. *Nat Environ Pollut Technol* 21:1191–1199. <https://doi.org/10.46488/NEPT.2022.v2i103.024>
- Melak F, Du Laing G, Ambelu A, Alemayehu E (2016) Application of freeze desalination for chromium (VI) removal from water. *Desalination* 377:23–27. <https://doi.org/10.1016/j.desal.2015.09.003>
- Min D, Cheng L, Zhang F, Huang XN, Li DB, Liu DF, Lau TC, Mu Y, Yu HQ (2017) Enhancing extracellular electron transfer of *Shewanella oneidensis* MR-1 through coupling improved flavin synthesis and metal-reducing conduit for pollutant degradation. *Environ Sci Technol* 51:5082–5089. <https://doi.org/10.1021/acs.est.6b04640>
- Miyawaki O, Inakuma T (2021) Development of progressive freeze concentration and its application: a review. *Food Bioprocess Technol* 14:39–51. <https://doi.org/10.1007/s11947-020-02517-7>
- Moharramzadeh S, Ong SK, Alleman J, Cetin KS (2021) Parametric study of the progressive freeze concentration for desalination. *Desalination* 510:115077. <https://doi.org/10.1016/j.desal.2021.115077>
- Munoz-Cupa C, Hu Y, Xu C, Bassi A (2021) An overview of microbial fuel cell usage in wastewater treatment, resource recovery and energy production. *Sci Total Environ* 754:142429. <https://doi.org/10.1016/j.scitotenv.2020.142429>
- Najim A (2022) A review of advances in freeze desalination and future prospects. *NPJ Clean Water* 5:15
- Najim A, Krishnan S (2022) Experimental and theoretical investigation of a novel system for progressive freeze-concentration based desalination process. *Chem Eng Process Process* 173:108821. <https://doi.org/10.1016/j.cep.2022.108821>
- Najim A, Krishnan S (2023) Experimental study on progressive freeze-concentration based desalination employing a rectangular channel crystallizer. *Environ Sci (Camb)* 9:850–860. <https://doi.org/10.1039/d2ew00892k>
- Ni G, Christel S, Roman P, Wong ZL, Bijmans MFM, Dopson M (2016) Electricity generation from an inorganic sulfur compound containing mining wastewater by acidophilic microorganisms. *Res Microbiol* 167:568–575. <https://doi.org/10.1016/j.resmic.2016.04.010>
- Nielsen G, Coudert L, Janin A, Blais JF, Mercier G (2019) Influence of organic carbon sources on metal removal from mine impacted water using sulfate-reducing bacteria bioreactors in cold climates. *Mine Water Environ* 38:104–118. <https://doi.org/10.1007/s10230-018-00580-3>
- Obileke KC, Onyeaka H, Meyer EL, Nwokolo N (2021) Microbial fuel cells, a renewable energy technology for bio-electricity

- generation: a mini-review. *Electrochem Commun* 125:107003. <https://doi.org/10.1016/J.ELECOM.2021.107003>
- Otero FJ, Yates MD, Tender LM (2019) Extracellular electron transport in *Geobacter* and *Shewanella*: a comparative description. Microbial electrochemical technologies. CRC Press, Boca Raton, pp 3–14
- Peng X, Tang T, Zhu X, Jia G, Ding Y, Chen Y, Yang Y, Tang W (2017) Remediation of acid mine drainage using microbial fuel cell based on sludge anaerobic fermentation. *Environ Technol* 38:2400–2409. <https://doi.org/10.1080/09593330.2016.1262462>
- Popugaeva D, Allen E, Corriveau M, Govindaraj S, Kreyman K, Ray AK (2023) The application of freezing technology for zinc removal from Faro pit mine-impacted water, Yukon, Canada. *Cold Reg Sci Technol* 213:103922. <https://doi.org/10.1016/j.coldregions.2023.103922>
- Popugaeva D, Allen E, Corriveau M, Govindaraj S (2021) Purification of mine-impacted water by freezing: laboratory data analysis and mathematical modeling. *Proc, IWA Young Water Professionals Canadian National Conference*
- Raghad J, Amin AS, Asaad AT (2016) Bioaccumulation of cadmium and lead by *Shewanella oneidensis* isolated from soil in Basra governorate, Iraq. *Afr J Microbiol Res* 10:370–375. <https://doi.org/10.5897/ajmr2016.7912>
- Samsuri S, Amran NA, Yahya N, Jusoh M (2016) Review on progressive freeze concentration designs. *Chem Eng Commun* 203:345–363
- Shone RDC (1987) The freeze desalination of mine waters. *J S Afr Inst Min Metall* 87:107–112
- Stefanova A, Angelov A, Bratkova S, Genova P, Nikolova K (2018) Influence of electrical conductivity and temperature in a microbial fuel cell for treatment of mining waste water. *Annals of “Constantin Brancusi,” Univ of Targu Jiu, Engineering Series*, pp 18–24. [https://www.utgjiu.ro/rev\\_ing/pdf/2018-3/02\\_A.STEFANOVA%20-INFLUENCE%20OF%20ELECTRICAL%20CONDUCTIVITY%20AND%20TEMPERATURE%20IN%20A%20MICROBIAL%20FUEL%20CELL%20FOR%20TREATMENT%20OF%20MINING%20WASTE%20WATER.pdf](https://www.utgjiu.ro/rev_ing/pdf/2018-3/02_A.STEFANOVA%20-INFLUENCE%20OF%20ELECTRICAL%20CONDUCTIVITY%20AND%20TEMPERATURE%20IN%20A%20MICROBIAL%20FUEL%20CELL%20FOR%20TREATMENT%20OF%20MINING%20WASTE%20WATER.pdf)
- Sulonen MLK, Kokko ME, Lakaniemi AM, Puhakka JA (2014) Electricity generation from tetrathionate in microbial fuel cells by acidophiles. *J Hazard Mater* 284:182–189. <https://doi.org/10.1016/j.jhazmat.2014.10.045>
- The Government of Canada (2022) Metal mining effluent regulations
- Vélez-Pérez LS, Ramirez-Nava J, Hernández-Flores G, Talavera-Mendoza O, Escamilla-Alvarado C, Poggi-Varaldo HM, Solorza-Feria O, López-Díaz JA (2020) Industrial acid mine drainage and municipal wastewater co-treatment by dual-chamber microbial fuel cells. *Int J Hydrogen Energy* 45:13757–13766. <https://doi.org/10.1016/j.ijhydene.2019.12.037>
- Wang X, Li J, Wang Z, Tursun H, Liu R, Gao Y, Li Y (2016) Increasing the recovery of heavy metal ions using two microbial fuel cells operating in parallel with no power output. *Environ Sci Pollut Res* 23:20368–20377. <https://doi.org/10.1007/s11356-016-7045-y>
- Wijewardena D (2018) Toxic and precious metals removal from wastewater using freeze concentration and electrodeionization. Dissertation, Lakehead University
- Xie GR, Choi CS, Lim BS, Chu SX (2020) Continuous removal of heavy metals by coupling a microbial fuel cell and a microbial electrolytic cell. *Membr Water Treat* 11:283–294. <https://doi.org/10.12989/mwt.2020.11.4.283>
- Xu C, Kolliopoulos G, Papangelakis VG (2022) Industrial water recovery via layer freeze concentration. *Sep Purif Technol* 292:121029. <https://doi.org/10.1016/j.seppur.2022.121029>
- Yin Y, Yang Y, de Lourdes Mendoza M, Zhai S, Feng W, Wang Y, Gu M, Cai L, Zhang L (2017) Progressive freezing and suspension crystallization methods for tetrahydrofuran recovery from Grignard reagent wastewater. *J Clean Prod* 144:180–186. <https://doi.org/10.1016/j.jclepro.2017.01.012>
- Yin Y, Liu C, Zhao G, Chen Y (2022) Versatile mechanisms and enhanced strategies of pollutants removal mediated by *Shewanella oneidensis*: a review. *J Hazard Mater* 440:129703. <https://doi.org/10.1016/j.jhazmat.2022.129703>
- Youssef PG, Al-Dadah RK, Mahmoud SM (2014) Comparative analysis of desalination technologies. *Energy Procedia* 61:2604–2607
- Zinicovscaia I, Safonov A, Boldyrev K, Gundorina S, Yushin N, Petuhov O, Popova N (2020) Selective metal removal from chromium-containing synthetic effluents using *Shewanella xiamenensis* biofilm supported on zeolite. *Environ Sci Pollut Res* 27:10495–10505. <https://doi.org/10.1007/s11356-020-07690-y>
- Zinicovscaia I, Yushin N, Grozdov D, Abdusamadzoda D, Safonov A, Rodlovskaya E (2021) Zinc-containing effluent treatment using *Shewanella xiamenensis* biofilm formed on zeolite. *Materials* 14:1760. <https://doi.org/10.3390/ma14071760>

Springer Nature or its licensor (e.g. a society or other partner) holds exclusive rights to this article under a publishing agreement with the author(s) or other rightsholder(s); author self-archiving of the accepted manuscript version of this article is solely governed by the terms of such publishing agreement and applicable law.